Effects of Substituents and Solvents on the Electronic Spectra of 9,10-Dihydro-9,10-*o*-benzenoanthracene-1,4-diones: Intramolecular Charge Transfer

Nobuya KITAGUCHI†
Department of Chemistry, Faculty of Science, Kyoto University,
Kitashirakawa, Sakyo-ku, Kyoto 606
(Received August 2, 1988)

Electronic spectra of substituted 9,10-dihydro-9,10-*o*-benzenoanthracene-1,4-diones (triptycenequinones) in various solvents and that of benzo- and dibenzotriptycenequinones were investigated in this paper. Intramolecular charge-transfer (CT) bands ware observed in triptycenequinone system as a result of intramolecular interaction between benzene ring and benzoquinone moiety. Substituents on the benzene rings strongly affected the CT bands. Electron-donating groups gave absorption maxima at long wavelength. Naphthalene ring gave similar but stronger CT bands than benzene ring. Hammett σ^+ value of substituents gave good linear relationship with the energy of the CT bands. Calculations of reduced charge matrix of triptycenequinones by extended Hückel theory showed that the charge of aromatic ring(s) were transferred to benzoquinone moiety accompanying HOMO–LUMO excitation. Especially, absorption maxima of the methyl-substituted triptycenequinones gave good correlation with the amounts of charge transferred from benzene ring to benzoquinone moiety. These analysis confirmed clearly CT character of the absorption maxima of triptycenequinones. However, solvent effect of these CT bands maxima is not so clear as the substituent effect.

The problem of transannular π–π interaction among neighboring benzene rings in triptycene system is of increasing interest in organic chemistry.[1–10]

On the electronic state of triptycene, Bartlett explained its absorption spectrum by the cross-ring interaction as follows.[1,2]

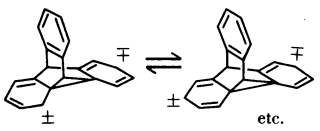

Structure **A**

Wit[3] prepared a variety of heterocyclic triptycenes and reported that the energy of their absorption maxima correlated to the energy calculated by Hückel MO including "through-space resonance" as follows. This fact suggests that "through-space" interactions may exist in triptycene system.

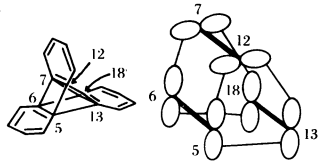

Structure **B**

Investigation of the intramolecular orbital interactions was reported to reveal differences in the nature of the interactions between the three benzene rings of triptycene based on electronic transmission spectroscopy.[4] It was also reported that the LUMO of triptycene is expected to have the significant contribution of the through-bond interaction, on the contrary to the HOMO which include the dominant through-space interaction.[5,6] 9,10-*o*-Benzenoanthracene-1,4,5,8-tetrone and 5,18:7,16:9,14-tri(*o*-benzeno)heptacen-1,4,6,8,10,13,15,17-octone derivatives were examined as electron acceptors in the intermolecular CT complex formation with 2-(1,3-dithiol-2-ylidene)-1,3-dithiole.[7] The properties of radical anions of triptycene bis- and tris-quinones have also been investigated.[8]

Furthermore, Murata observed charge-transfer (CT) transition for symmetry-forbidden CT interaction in methyl- or methoxy- substituted 9,10-*o*-benzenoanthracene-1,4-diones (triptycenequinones) (**1e—i**) using CH_2Cl_2 as a solvent.[9,10]

Thus, according to these previous results above, triptycene system itself has intramolecular through-space interaction between three benzene rings. It is interesting to investigate the change of such intramolecular interaction caused by introducing benzoquinone moiety into triptycene system and a variety of substituents into benzene rings.

In this paper, effect of substituents, (methyl, acetylamino, dichloro) on the absorption spectra of triptycenequinones (**1a—d**) as well as benzotriptycenequinone (**3**), dibenzotriptycenequinone (**4**) and non-aromatic analogue (**2**) will be reported together with solvent effect on substituted triptycenequinones **1a—d**. Some results of those quinones were discussed in view of charge flow induced by HOMO–LUMO excitation calculated with Extended Hückel Theory (EHT).

† Present address: Bio-science Laboratory, Life Science Laboratories, Asahi Chemical Industry Co., Ltd., Samejima 2-1, Fuji city, Shizuoka 416. A part of this work was done in this laboratory.

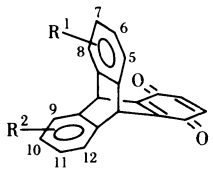

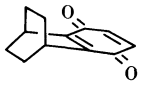

2

1a $R^1=R^2=H$
b R^1=6-Me, $R^2=H$
c R^1=6-NHCOMe, $R^2=H$
d R^1=5-Cl, R^2=9-Cl
e R^1=5-Me, $R^2=H$
f R^1=5, 8-Me_2, $R^2=H$
g R^1=6, 7-Me_2, $R^2=H$
h R^1=5, 8-$(OMe)_2$, $R^2=H$
i R^1=6, 7-$(OMe)_2$, $R^2=H$

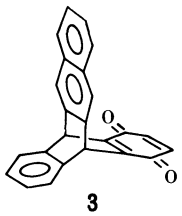

3

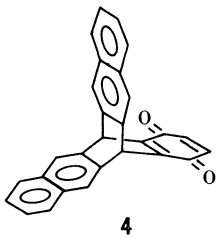

4

dichloro (**1d**), gave shorter absorption maximum than unsubstituted triptycenequinone (**1a**). So, these maxima can be regarded as the result of CT interaction between benzene ring and benzoquinone moiety (further analysis is given in the part of Discussion). Such maxima could not be observed by intermolecular interaction between **2** and benzene (Fig. 1). Intermolecular CT band of **2** and benzene appeared in the region of 280—300 nm (Fig. 2), far shorter wavelength than that of triptycenequinones. The 280—300 nm band of **2** in benzene is compatible to the reported CT band between 1,4-benzoquinone and benzene.[15] Furthermore, the absorption maxima of triptycenequinones are completely different from those observed in the electronic spectrum of cyclophanequinone **5**. The latter showed the CT band at 340 nm arising from interaction between benzene and 1,4-benzoquinone moieties.[16]

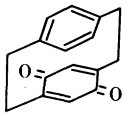

5

Result

1. Absorption Spectra of the Substituted Triptycenequinones. Figure 1 shows the absorption spectra (λ; wavelength, ε; absorptivity) of triptycenequinones **1a—d** in $CHCl_3$ and that of non aromatic derivative **2** in C_6H_6. The triptycenequinones have characteristic absorption maxima (ε; 190—360) in the region of 390—430 nm. Substitution with electron-donating groups, methyl (**1b**) or acetylamino (**1c**) group, gave absorption maxima at longer wavelength. To the contrary, substitution with electron-withdrawing group,

Consequently, it can be concluded that these absorption maxima of **1a—d** observed in the region of 390—430 nm are of characteristic in the triptycenequinone system, and that these bands are due to intramolecular CT interaction.

2. Solvent Dependency of the Absorption Maxima in Triptycenequinones 1a—d. To make clear CT character of the absorption maxima in triptycenequinone system, solvent dependency of absorption band of **1a** was examined in 14 solvents. Three solvents were used in the case of **1b—d**. The results are summarized in Tables 1 (**1a**) and 2 (**1b—d**). As a

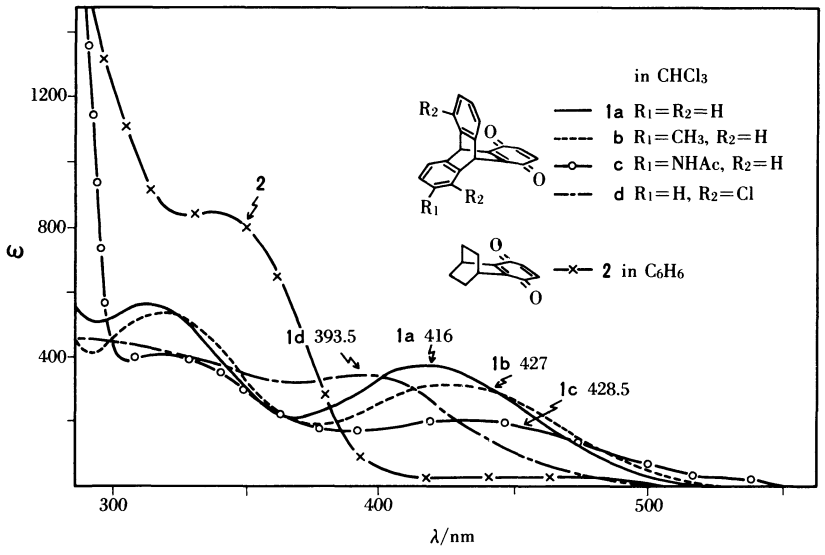

Fig. 1. Absorption spectra of **1a—d** in $CHCl_3$ and **2** in C_6H_6.

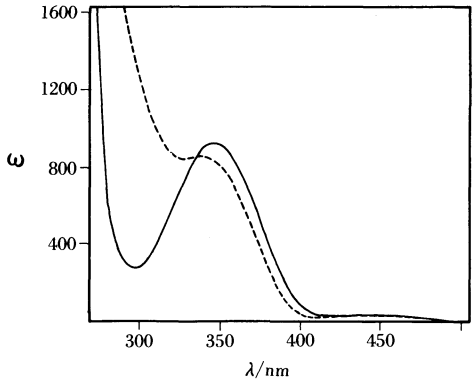

Fig. 2. Absorption spectra of **2** in $CHCl_3$ (solid line) and in C_6H_6 (dashed line).

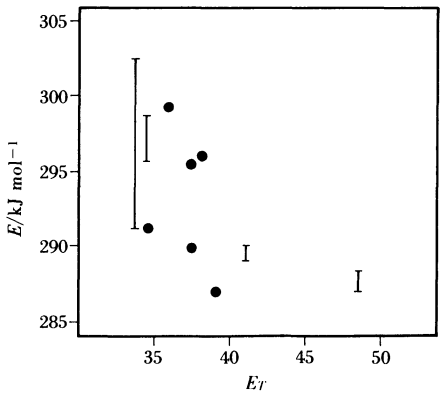

Fig. 3. Solvent dependency of the characteristic band of **1a**.

Table 1. Solvent Dependency of the Characteristic Bands of Triptycenequinone **1a**

Solvent	E_T	λ/nm (log ε)
$C_6H_5CH_3$	33.9	395—410 (shoulder)
C_6H_6	34.5	410 (2.50)
Et_2O	34.6	400.0—403.5
Dioxane	36.0	399.5
THF	37.4	404.5
C_6H_5Cl	37.5	412
$EtOCOCH_3$	38.1	403
$CHCl_3$	39.1	416 (2.56)
CH_2Cl_2	41.1	412—413
Acetone	42.2	403
DMF	43.8	404.0—406.5
CH_3CN	46.0	403—404 (2.50)
2-Propanol	48.6	414—416
Acetic acid	52.0[a]	407.5—410.0

a) Estimated from its Z value.

Table 2. Characteristic Bands of Substituted Triptycenequinones **1b—d**

Quinone	Solvent	Wavelength (nm)	log ε
1b	C_6H_6	421	2.47
	$CHCl_3$	427	2.50
	CH_3CN	412	2.45
1c	C_6H_6	428	2.29
	$CHCl_3$	428.5	2.28
	CH_3CN	423.5	2.29
1d	C_6H_6	—[a]	
	$CHCl_3$	393.5	2.54
	CH_3CN	381	2.51

a) Shoulder.

parameter of solvent polarity, Dimroth's E_T values[17,18] were adopted instead of Kosower's Z values by two reasons. Main reason is that Z values of some solvents have not been reported yet. The other reason is that E_T values are determined from intramolecular CT transition of diphenyl betaines **6**. Meanwhile, Z values are determined from closely-contacted interionic CT interaction between iodide anions and pyridium cations. Good linear correlation was obtained between E_T value and Z value (Z=1.259E_T+13.76).[18] In the case of the solvents whose E_T- and Z-values were both reported, analysis with Z values gave similar results as E_T values.

No clear solvent dependency can be recognized as given in Tables 1 and 2. However, among the solvents shown in Table 1, acetone, DMF, and acetonitrile are classified as "dissociating solvents" and acetic acid is classified as "associating solvent",[19-21] because these solvents affect excitation of compounds in a little different way from other solvents. When those dissociating and associating solvents are excluded, the energy of the absorption maximum (E) somehow tends to decrease with increase of solvent polarity E_T as given in Fig. 3. This tendency may support the CT character of the absorption maxima in triptycenequinone system.

Standing on another viewpoint, unclear solvent dependency of the absorption maxima can be speculated to be due to the following two reasons. One is that the charge separation of excited state in triptycenequinones is not so large as that in the compound (**6**) used for determination of E_T values. The other reason is that the character of n-π^* transition of carbonyl group (blue shift when solvent polarity increases) might complex with the CT character (red shift when solvent polarity increases).

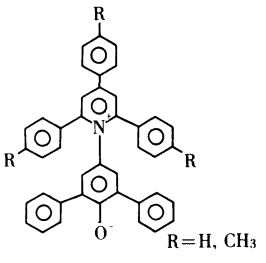

6

3. Absorption Spectra of Benzotriptycenequinone 3 and Dibenzotriptycenequinone 4. Naphthalene-ring-incorporated triptycenequinone analogues, benzotri-

ptycenequinone **3** and dibenzotriptycenequinone **4**, showed quite different spectra from that of a 1:1 mixture of **2** and naphthalene (Fig. 4) as in the case of benzene derivatives **1a—d**. The λ_{max}'s were 411—412 nm (ε= 468) in **3** and 400.5 nm (708) in **4**. The ε of the absorption maximum of **4** were larger than that of **3**, so it can be said that additional naphthalene ring may raise degree of intramolecular interaction. These absorption maxima in the region of 400—420 nm were very similar to those of **1a—d**, but had a little larger ε.

However, in the region of 470—550 nm, the quinones **3** and **4** have fairly strong absorption bands (ε's at 500 nm were ca. 100 and 160, respectively) compared with **1a—d**. The ε_A's—apparent absorptivity—of these absorption maxima of **3** and **4** did not depend on the concentration of these compounds. So, these 470—550 nm bands can be considered to come from *intramolecular* process.

Although a 1:1 mixture of **2** and naphthalene at low concentration showed no band arising from the intermolecular interaction between these two molecules ([**2**]=4.83×10^{-3} mol dm^{-3}, [naphthalene]=5.13×10^{-3} mol dm^{-3}), a highly concentrated 1:100 mixture of **2** and naphthalene ([**2**]=1.02×10^{-2} mol dm^{-3}, [naphthalene]=1.4 mol dm^{-3}) showed a weak band at 450 nm (Fig. 5). Based on these observations and the results of triptycenequinones described above, the strong and large absorption maxima of **3** and **4** in the region around 400—550 nm can be assigned to the intramolecular CT transition between naphthalene ring and benzoquinone moiety.

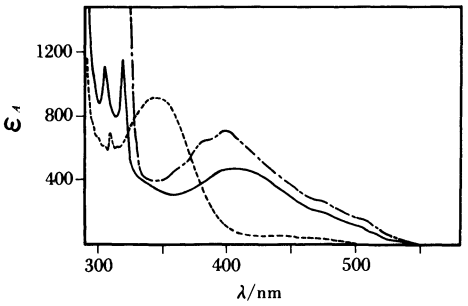

Fig. 4. Absorption spectra of **3** (——), **4** (— — — —), and 1:1 mixture of **2** and naphthalene (----) in $CHCl_3$. In the region of longer wavelength than 400 nm, [**2**]=4.83×10^{-3} mol dm^{-3}, and [naphthalene]=5.13×10^{-3} mol dm^{-3}. In the region of shorter wavelength than 400 nm, 4.83×10^{-4} mol dm^{-3} and 5.13×10^{-4} mol dm^{-3}, respectively.

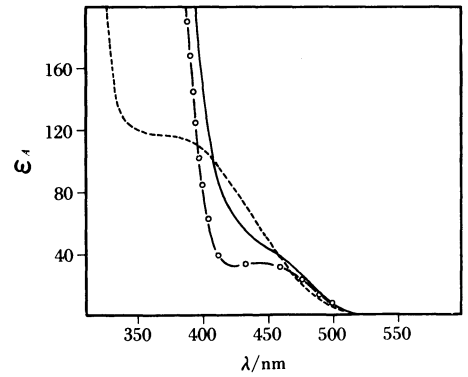

Fig. 5. Absorption spectra of 1:100 mixture of **2** (1.02×10^{-2} mol dm^{-3}) and naphthalene (1.4 mol dm^{-3}) (——), 1:100 mixture of 1,4-benzoquinone (1.02×10^{-2} mol dm^{-3}) and naphthalene (9.99×10^{-1} mol dm^{-3} (--------), and **2** itself (—O—O—). Solvent; $CHCl_3$.

4. Reduced Charge Calculations by EHT.[22,23] The calculation of the charges of each atom (reduced charge matrix, molecular orbital-atom) was carried out in HOMO and in LUMO of triptycenequinones **1a—d** by EHT in order to investigate more details on the absorption maxima.

The probable conformations of the triptycenequinones were calculated by molecular mechanics theory (see Experimental section), then reduced charge matrix were obtained by EHT calculation. As a result of these calculations, the overlap integrals and overlap populations between homoconjugative atoms (carbon atoms vicinal to bridgehead carbons) were found to be significant in these triptycenequinones. Reduced charge matrix in HOMO and in LUMO (one electron in each MO) and differences between these two MOs (Δ_{L-M}: LUMO minus HOMO, considered as S_0–S_1 excitation) are given in Table 3 in the case of unsubstituted triptycenequinone **1a**. In the case of other triptycenequinones (**1b—i**, **3**, **4**), only the summations of Δ_{L-M} in each moiety [$\sum$(moiety Δ_{L-H})] are tabulated in Table 4. Numbering of atoms are shown in the following structure. Here, [A] represents mainly-substituted aromatic ring, [B]; another aromatic ring, [Q]; benzoquinone moiety, and [BH]; bridgehead carbon atom.

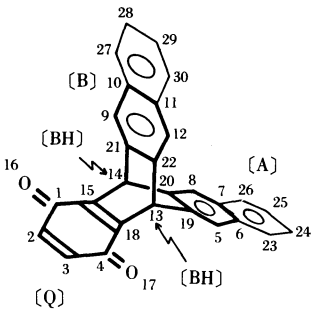

Structure C

As shown in Tables 3 and 4, $\sum(\Delta_{L-M})$ in each moiety are all negative in ring A and in sum of A and B (A+B), but all positive in ring Q, suggesting that HOMO-LUMO excitation in triptycenequinone system involves charge transfer from aromatic ring (ring A and/or B) to benzoquinone moiety (ring Q). That is, rings A and B can be considered as electron donor,

Table 3. Reduced Charge Matrix and Population Change Δ_{L-H} in **1a** Calculated by EHT

Moiety	Atom number	Reduced charge matrix		Population change Δ_{L-H}
		HOMO	LUMO	
A	20	0.0761	0.0223	−0.0538
	19	0.0738	0.0033	−0.0706
	5	0.0511	0.0059	−0.0452
	6	0.0332	0.0043	−0.0289
	7	0.0759	0.0069	−0.0690
	8	0.0042	0.0069	0.0027
	Σ(A)	0.3143	0.0496	−0.2647
B	22	0.0017	0.0057	0.0040
	21	0.0078	0.0139	0.0061
	9	0.0026	0.0086	0.0060
	10	0.0065	0.0043	−0.0022
	11	0.0009	0.0027	0.0018
	12	0.0075	0.0030	−0.0045
	Σ(B)	0.0270	0.0382	0.0112
BH	13	0.0662	0.0059	−0.0603
	14	0.0062	0.0297	0.0235
	Σ(BH)	0.0724	0.0356	−0.0368
Q	15	0.0718	0.1888	0.1170
	1	0.0151	0.2282	0.2131
	16	0.0210	0.0220	0.0010
	2	0.1121	0.0810	−0.0311
	3	0.0365	0.1099	0.0734
	17	0.1662	0.0442	−0.1220
	4	0.1522	0.1577	0.0055
	18	0.0060	0.0359	0.0299
	Σ(Q)	0.5809	0.8677	0.2868

Table 4. Summation of Population Change in Each Moiety Σ(moiety Δ_{L-H})[a] of Triptycenequinones

Quinone	Σ(moiety Δ_{L-H})				
	A	B	BH	Q	A+B
1a	−0.2647	0.0112	−0.0368	0.2868	−0.2535
1b[b]	−0.6640	0.0115	0.0167	0.6510	−0.6525
1c[b]	−0.2508	−0.1112	−0.0746	0.5011	−0.3620
1d	−0.2064	−0.0189	−0.0383	0.2558	−0.2253
1e	−0.2940	−0.0557	−0.0694	0.5357	−0.3497
1f	−0.3460	0.1036	0.0536	0.2008	−0.2424
1g	−0.7467	0.0100	0.0182	0.7639	−0.7367
1h	−0.1569	−0.0580	−0.0283	0.3340	−0.2149
1i	−0.0708	−0.1785	−0.0574	0.3498	−0.2493
3	−0.2783	−0.1307	−0.0422	0.4810	−0.4090
4	−0.2765	−0.1008	−0.0559	0.4324	−0.3772

a) Reduced net AO population was normalized to one electron occupation. b) Two of asymmetrical triptycenequinone derivatives (6-Me, **1b** and 6-NHCOCH$_3$, **1c**) were calculated as 7-Me and 7-NHCOCH$_3$ derivatives, respectively, for convenience sake.

and ring Q as electron acceptor, so charge is calculated to be transferred from mainly ring Q accompanying HOMO–LUMO excitation.

For comparison, reduced charge matrix of 9,10-dihydro-1,4-anthracenedione **7a** and its 6-methyl derivative **7b** were calculated by the same method as in the case of triptycenequinones. The results are summarized in Table 5. In both cases, sums of population change are all positive in ring A and "Bridge Head", and all negative in ring Q, as opposed to sterically rigid triptycenequinone system. So charge flow in

Table 5. Summation of Population Change in Each Moiety Σ(moiety Δ_{L-H})[a] of **7a, b**

Quinone	Σ(moiety Δ_{L-H})		
	A	BH	Q
7a	0.2804	0.2237	−0.5830
7b	0.3113	0.1808	−0.5651

a) Reduced net AO population was normalized to one electron occupation.

1a—i, **3**, and **4** can be considered as characteristic of these triptycenequinones.

More details are described in the part of "Discussion".

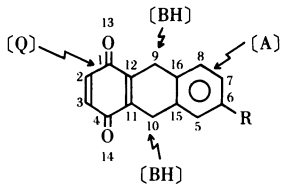

7a R=H
b R=CH_3

Discussion

Substituent effects and the CT character of absorption maxima in triptycenequinone system are analyzed using Hammett σ^+ constant and population change calculated by EHT as parameters.

The absorption maxima in triptycenequinone system could be analyzed quantitatively by the linear free energy relationship. When the positions 6, 7, 10, 11 of **1a—d** are assumed to be *p*-position and the positions 5,8,9,12 are *m*-position, the energy of these bands in three solvents (CH_3CN, $CHCl_3$, and C_6H_6) gave straight lines in Hammett plot using σ^+ values[24,25] (Fig. 6). Furthermore the absorption maxima of other triptycenequinones **1e—i**, obtained in CH_2Cl_2 previously by Murata et al.,[8,9] were analyzed with similar Hammett plot as shown in Table 6 and Fig. 7.

As shown in Figs. 6 and 7, clear linear correlation was obtained between energy of absorption maximum and σ^+, not σ. It suggests that benzene ring has a little cationic (electron-donating) character in the course of S_0–S_1 excitation, and then that these absorption maxima in triptycenequinones may reflect the presence of the charge-transfer electron transition from neighboring aromatic rings to 1,4-benzoquinone moiety.

This interpretation was also supported by EHT calculations of reduced charge. Sum of population change $\Sigma(\Delta_{L-H})$ in each moiety, benzene rings A and B, bridge head BH, and benzoquinone Q, are compared with energy of the absorption maxima in substituted triptycenequinones **1a—i**, **3**, and **4**. Population changes

Table 6. Energy of the Characteristic Bands[8,9] of Triptycenequinones **1a**, **b**, and **1e—i** in CH_2Cl_2 with Hammett Constant[a]

Quinone	E/kJ mol^{-1}	σ^+	σ
1a	288.3	0	0
1b	282.4	−0.26	−0.17
1e	287.9	−0.065	−0.069
1f	289.5	−0.13[b]	−0.138[b]
1g	273.2	−0.622[b]	−0.34[b]
1h	287.0	0.10[b]	0.23[b]
1i	253.6	−1.30[b]	0.536[b]

a) σ^+ values of **1c** and **1d** is −0.25 and 0.80, respectively.
b) Calculated as summation of σ or σ^+ values of single substituent.

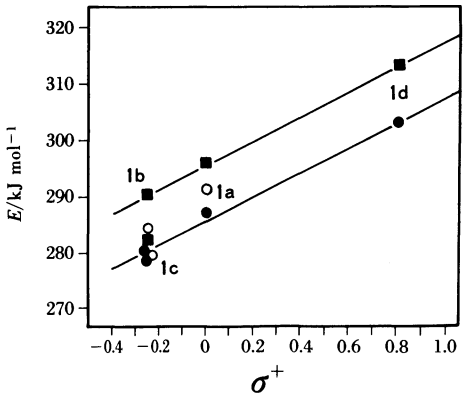

Fig. 6. Hammett plot: the energies of the absorption maxima in **1a—d** vs. σ^+ values. Closed circle; in $CHCl_3$. Closed square; in CH_3CN. Open circle; in C_6H_6.

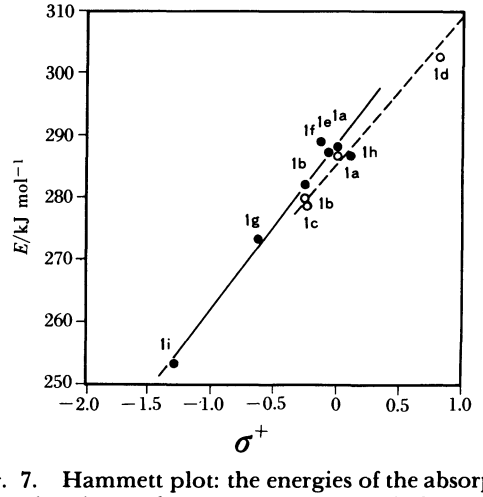

Fig. 7. Hammett plot: the energies of the absorption maxima in **1a—i** vs. σ^+ values. Open circle; **1a—d** in $CHCl_3$. Closed circle; **1a**, **1b**, and **1e—i** in CH_2Cl_2.[8,9]

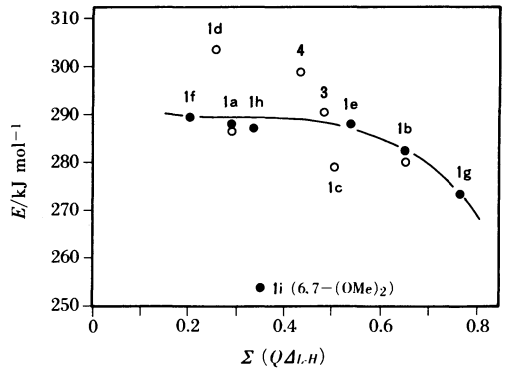

Fig. 8. A plot of sum of population change in moiety Q against absorption maximum energy. Open circle; **1a—d**, **3**, and **4** in $CHCl_3$. Closed circle; **1a**, **1b**, and **1e—i** in CH_2Cl_2.

in moiety Q[$\Sigma(Q\Delta_{L-H})$] are plotted against energy of the absorption maxima (Fig. 8). $\Sigma(Q\Delta_{L-H})$ shows good correlation to absorption maxima, especially in the case of methyl substituted triptycenequinones. Population change in moiety A and B [$\Sigma((A+B)\Delta_{L-H})$] gave similar results as $\Sigma(Q\Delta_{L-H})$.

Thus, analysis of S_0–S_1 transition by MO calculation strongly suggests that absorption maxima of triptycenequinones can be attributed to the charge transfer from benzene ring to quinone moiety, as well as analysis by Hammett plots. This charge transfer may be occurred mainly "through-space" because the quite different results were obtained by the calculation of **7a,b**, which can be considered to include much less "through-space" interaction than triptycenequinones because of their planar conformation.

The quite different population change of **7a,b** compared to triptycenequinones may result mainly from the difference of overlap integrals. The overlap populations between atomic orbitals of the carbon atoms adjacent to bridgehead carbons were much larger in triptycenequinones than in **7a,b**. Those in **7a,b** were almost zero. So, triptycenequinones may have much stronger through-space interaction than **7a,b**. Such difference was explicitly shown by the population change in bridgehead carbon atoms, which can interact with the benzoquinone moiety mainly by through-bond interaction. **7a,b** gave much larger $\Sigma(BH\Delta_{L-H})$ than triptycenequinones (Tables 4 and 5).

The summation of reduced charge of all atoms in benzoquinone moiety Q changed from 0.5809 to 0.8677 in **1a** and from 0.8603 to 0.2773 in **7a** through S_0–S_1 excitation. In the course of that excitation, population change of carbonyl groups was calculated to be 0.2131 for carbon atom and 0.0010 for oxygen atom in **1a**, and −0.2431 for C and −0.0436 for O in **7a**. So, the difference of population change $\Sigma(Q\Delta_{L-H})$ mainly came from the difference of the population change of carbonyl carbons. In the case of **7a,b**, the electron in S_0 state may exist mainly on the benzoquinone moiety, especially on carbonyl carbon atoms, and may diffuse into whole molecule by through-bond interaction in the course of excitation to S_1 state. Further, according to population change of carbonyl oxygen atoms described above, S_0–S_1 excitation of triptycenequinones might have somewhat π–π^* character, on the other hand, that of **7a,b** might have less π–π^* and more n–π^* character, because more electron on carbonyl oxygen atoms may diffuse in S_1 state in **7a,b** than in triptycenequinones. The cause of the different population change is still unclear and more investigation is required for exact explanation.

Based on good linear correlation between absorption maximum and σ^+ constant, the absorption maximum can be expected by Hammett plot such as Fig. 7. Furthermore, as far as methyl-substituted triptycenequinones, the absorption maximum may be expected also by such simple EHT calculation. However, neither $\Sigma(A\Delta_{L-H})$ nor $\Sigma(Q\Delta_{L-H})$ of 6,7-dimethoxy (**1i**), acetylamino (**1c**), chloro (**1d**), and dibenzo (**4**) derivatives gave clear correlation to the absorption maximum, compared with Hammett σ^+ constants. It is speculated as due to the effect of lone-pair electrons which is not perhaps involved sufficiently within this EHT calculation.

Experimental

Apparatus for Measurements. Electronic spectra were taken with a Shimadzu UV-200 spectrometer. ^{1}H NMR spectra were taken with a JEOL PS-100MHz spectrometer in suitable solvents using TMS as the internal standard.

Solvents. For absorption spectra measurements, solvents were dried with appropriate desiccant, and distilled.

Quinones. **1a—d**, **3**, **4** were prepared according to the previously reported method[1,10] with some modification. Corresponding anthracenes were synthesized (for **1b—d**) or purchased (for **1a**). Naphthacene (for **3**) and pentacene (for **4**) were synthesized as described later. All polyacenes were purified by recrystallization. Triptycenequinones were synthesized as follows. After Diels-Alder reaction of 1,4-benzoquinone and a polyacene, the adduct was precipitated with cooling to room temperature. The precipitate was recrystallized from benzene and then treated with HBr in acetic acid to give the corresponding hydroquinone. The hydroquinone was then oxidized to the corresponding triptycenequinone with potassium bromate in acetic acid. Detail conditions of Diels-Alder reaction were as follows [given as target compound, polyacene used (g), 1,4-benzoquinone used (g), solvent (ml), refluxing period, yield (g)]: **1a**, 10.8, 7.3, xylene 65, 3 h, 13.8; **1b**, 5.3, 3.6, xylene 65, 3 h, 5.9; **1c**, 2.1, 1.6, toluene 25, 3 h, 3.0; **1d**, 4.5, 2.1, xylene 30, 3.5 h, 2.8; **3**, 3.0, 1.4, xylene 25 (under N_2), 30 min, 2.1, 3.8; **4**, 1.9, 0.8, xylene 14 (under N_2), 20 min, 0.5.

The physical properties of **1a—d**, **3**, **4** were as follows.

1a: Yellow prisms recrystallized from $CHCl_3$, mp 289—294 °C (decomp) (lit, 292—296 °C). ^{1}H NMR ($CDCl_3$): δ=5.76 (s, 2H), 6.56 (s, 2H), 6.96—7.20 (m, 4H), 7.30—7.56 (m, 4H). IR (KBr): ν_{CO}=1655 cm^{-1}. UV ($CHCl_3$): λ_{max}= 416 nm (ε=357), 311 (513), 244 (16500).

1b: Yellow crystals from benzene, mp 165.2—168.4 °C (slightly decomp)(sealed tube). ^{1}H NMR ($CDCl_3$): δ=2.57 (s, 3H), 6.51 (s, 2H), 7.40 (s, 2H), 7.66 (m like d, 1H), 7.80—8.00 (m, 2H), 8.14 (s, 1H), 8.16—8.38 (m, 3H). IR (KBr): ν_{CO}=1660 cm^{-1}, $\nu_{C=C}$=1598 cm^{-1}. MS m/z=298 (M^+), 280 (M−CO). UV ($CHCl_3$): λ_{max}=427 nm (ε=316), 320 (526), 279 (3060), 261 (sh, 15100), 255 (15700). Found: C, 84.40; H, 4.81%. Calcd for $C_{21}H_{14}O_2$: C, 84.54; H, 4.73%.

1c: Orange yellow needles, mp 180.0—181.0 °C (decomp). ^{1}H NMR ($CDCl_3$): δ=2.10 (s, 3H), 5.66 (s, 2H), 6.50 (s, 2H), 6.87—7.03 (m, 3H), 7.1—7.4 (m, 4H, including NH), 7.60 (brs, 1H). IR (KBr): ν_{CO}=1652 cm^{-1} (broad), 1590, 1532, 1303. MS m/z=341 (M^+), 298 (M−Ac). UV ($CHCl_3$): λ_{max}=428.5 nm (ε=192), 321 (398), 257 (18400). Found: C, 77.28; H, 4.39; N, 3.88%. Calcd for $C_{22}H_{15}NO_3$: C, 77.41; H, 4.43; N, 4.10%.

1d: Yellow crystals from $CHCl_3$, mp at >240 °C slightly red and at 303—305 °C melted with decomposition (sealed tube). ^{1}H NMR ($CDCl_3$): δ=6.38 (s, 2H), 6.75 (s, 2H), 6.9—

7.3 (m, 4H), 7.3—7.6 (m like dd, 2H). IR (KBr): ν_{CO}= 1665 cm^{-1}, $\nu_{C=C}$=1590, 1570 cm^{-1}. MS m/z=354, 352 (M^+). UV ($CHCl_3$): λ_{max}=395.5 nm (ε=348), 298 (sh, 469), 278 (sh, 1000), 254.3 (14300). Found: C, 67.92; H, 2.79; Cl, 20.39%. Calcd for $C_{20}H_{10}O_2Cl_2$: C, 68.01; H, 2.85; Cl, 20.08%.

3: Orange yellow crystals, mp 210.5—211.0 °C (decomp) (sealed tube). ^1H NMR ($CDCl_3$): δ=5.86 (s, 2H), 6.58 (s, 2H), 7.0—7.2 (m, 2H), 7.4—7.6 (m, 4H), 7.6—7.8 (m, 2H), 7.78 (s, 2H). IR (KBr): ν_{CO}=1650 cm^{-1}, $\nu_{C=C}$=1585 cm^{-1}, ν=1305 cm^{-1}. MS m/z=335 (M+1), 334 (M^+). UV ($CHCl_3$) λ_{max}=411.5 nm (ε=460), 320.6 (1170), 306.8 (1120), 287.6 (4840), 262.5 (sh, 18900), 260 (19400), 243 (65600). Found: C, 86.13; H, 4.18%. Calcd for $C_{24}H_{14}O_2$: C, 86.21; H, 4.22%.

4: Orange crystals, mp 242—243 °C (sealed tube). ^1H NMR ($CDCl_3$): δ=5.92 (brs, 2H), 6.52 (s, 2H), 7.3—7.5 (m, 4H), 7.5—7.7 (m, 4H), 7.79 (s, 4H). IR (KBr): ν_{CO}=1655 cm^{-1}, $\nu_{C=C}$=1592 cm^{-1}, ν=1305 cm^{-1}. MS m/z=385 (M+1), 384 (M^+), 356, 355. UV ($CHCl_3$): λ_{max}=400.5 nm (ε=708). Found: C, 87.38; H, 4.22%. Calcd for $C_{28}H_{16}O_2$: C, 87.48; H, 4.20%.

2-Methylanthracene[11] and 1,5-Dichloroanthracene. 2-Methyl-9,10-anthraquinone and 1,5-dichloro-9,10-anthraquinone were reduced to the corresponding anthracenes with diborane in situ prepared by $NaBH_4$ and BF_3-etherate in diglyme. Crude substituted anthracene was purified by column chromatography on silica gel to give the mixture of the substituted anthracene and its 9,10-dihydro derivative. This mixture was oxidized with 1,4-benzoquinone (in the case of 2-methylanthracene) or chloranil (in the case of 1,5-dichloroanthracene) to give pure substituted anthracene.

2-Acethylaminoanthracene. 2-Amino-9,10-anthraquinone was reduced to 2-aminoanthracene in a similar manner as 6-methyl derivative. 2-Aminoanthracene obtained was acetylated with refluxing acetic anhydride to give 2-acetylaminoanthracene.

Naphthacene and Pentacene. 5,12-Naphthacenedione[12] and 6,13-pentacenedione[12] were prepared by condensation of $\alpha,\alpha,\alpha',\alpha'$-tetrabromo-*o*-xylene[13] and 1,4-naphthoquinone with NaI in dry *N,N*-dimethylformamide, and then reduced in a similar manner as in the case of substituted anthracenes.

5,6,7,8-Tetrahydro-5,8-ethano-1,4-naphthoquinone (2). Cyclohexadiene and 1,4-benzoquinone were condensed by Diels-Alder reaction. The adduct was rearranged to the corresponding hydroquinone, and then reduced with H_2/Pd-C. The hydroquinone was oxidized by $FeCl_3$. **2** was obtained as yellow crystals from hexane-benzene, mp 85.7—87.0 °C (sealed tube). ^1H NMR ($CDCl_3$): δ=1.2—1.6 (m, 4H), 1.6—1.9 (m, 4H), 3.34 (d, J=1 Hz, 2H), 6.71 (s, 2H). IR (KBr): ν_{CO}=1640 cm^{-1}, $\nu_{C=C}$=1585 cm^{-1}, ν=1303 cm^{-1}. MS m/z=188 (M^+), 186, 160 ($M-CH_2=CH_2$). UV ($CHCl_3$): λ_{max}=445 nm (ε=33), 348 (936), 254 (18000). Found: C, 76.41; H, 6.55%. Calcd for $C_{12}H_{12}O_2$: C, 76.57; H, 6.43%.

Purification of Quinones. In order to avoid the contamination with polyacenes, triptycenequinones **1a—d**, **3**, **4**, and nonaromatic quinone **2** were purified by column chromatography on silica gel twice and by recrystallization in a dark room.

EHT Calculations. A packaged soft for chemical calculations "CHEMLAB-II" supplied by MDL Inc. (U.S.A.) was used on VAX11/780, Digital Equipment Company. Molecular coordinates were calculated by "PRXBLD", one of suboptions in CHEMLAB-II, based on molecular mechanics. Extended Hückel calculations were carried out by "EHT" suboption.

The author wishes to express his grateful thanks to Professor Kazuhiro Maruyama for his guidance and invaluable discussions in this work. He is grateful to Dr. Yasuo Kubo for his helpful suggestions. He also thanks Dr. Tetsuo Otsuki, Dr. Yoshinori Naruta and Dr. Tatsuhisa Kato for fruitful discussion. The author wishes to thank Mr. Kazunori Toma for assistance of EHT calculations.

References

1) P. D. Bartlett, M. J. Ryan, and S. G. Cohen, *J. Am. Chem. Soc.*, **64**, 2649 (1942).
2) P. D. Bartlett and E. S. Lewis, *J. Am. Chem. Soc.*, **72**, 1005 (1950).
3) J. de Wit and H. Wynberg, *Tetrahedron*, **29**, 1379 (1973).
4) V. Balaji and K. D. Jordan, *Chem. Phys. Lett.*, **119**, 294 (1985).
5) S. Inagaki, T. Imai, and H. Kawata, *Chem. Lett.*, **1985**, 1191.
6) H. Iwamura and K. Makino, *J. Chem. Soc., Chem. Commun.*, **1978**, 720.
7) E. Lipczynska Kochany and H. Iwamura, *Chem. Lett.*, **1982**, 1075.
8) G. A. Russell and N. K. Suleman, *J. Am. Chem. Soc.*, **103**, 1560 (1981).
9) K. Yamamura, K. Nakasuji, I. Murata, and S. Inagaki, *J. Chem. Soc., Chem. Commun.*, **1982**, 396.
10) I. Murata, *Pure Appl. Chem.*, **55**, 323 (1983).
11) E. Clar, *Chem. Ber.*, **64**, 1676 (1931).
12) D. S. Bapt, B. C. Subba Rao, and M. K. Unni, *Tetrahedron Lett.*, **1960**, 15.
13) M. P. Cova, A. A. Deana, and K. Muth, *J. Am. Chem. Soc.*, **81**, 6459 (1959).
14) J. C. Bill and D. S. Tarbell, *Org. Synth.*, Coll. Vol. IV, 807 (1963).
15) L. J. Andrews and R. M. Keefer, *J. Am. Chem. Soc.*, **75**, 3776 (1953).
16) D. J. Cram and A. C. Day, *J. Org. Chem.*, **31**, 1227 (1966).
17) K. Dimroth, C. Reichardt, T. Siepmann, and F. Bohlmann, *Justus Liebigs Ann. Chem.*, **661**, 1 (1963).
18) K. Dimroth, C. Reichardt, and A. Schweig, *Justus Liebigs Ann. Chem.*, **669**, 95 (1963).
19) M. Senou and T. Arai, "Yuuki-kagaku-hannou Ni Okeru Youbaikouka," Sangyou Tosho, Tokyo (1975), Chap. 4.6—4.7.
20) E. M. Kosower, *J. Am. Chem. Soc.*, **80**, 3253, 3261, 3267 (1958).
21) C. Walling and P. J. Wagner, *J. Am. Chem. Soc.*, **86**, 3368 (1964).
22) R. Hoffmann, *J. Chem. Phys.*, **39**, 1397 (1963).
23) J. P. Lowe, "Quantum Chemistry," Academic Press, New York (1978), pp. 283—303.
24) S. L. Murov, "Handbook of Photochemistry," Marcel Dekker, Inc., New York (1973), Section 26, p. 200.
25) L. P. Hammett, "Physical Organic Chemistry," McGraw-Hill (1970), Chap. 11.